Predicting Avian Abundance Within and Across Tidal Marshes Using Fine-Scale Vegetation and Geomorphic Metrics

**Diana Stralberg · Mark P. Herzog · Nadav Nur ·
Karin A. Tuxen · Maggi Kelly**

Abstract Tidal marsh monitoring and restoration can benefit from the union of fine-scale remote sensing products and field-based survey data via spatial predictive models. As part of an interdisciplinary wetland monitoring project in San Francisco Bay, we developed a suite of 1-m pixel-level spatial metrics describing patterns in marsh vegetation and geomorphology for six sites across a large salinity gradient. These metrics, based on multi-spectral aerial imagery and derived vegetation maps, provided a basis for fine-scale spatial modeling of avian habitat potential. Using common yellowthroat (*Geothlypis trichas*), song sparrow (*Melospiza melodia*), and black rail (*Later-* *allus jamaicensis*) abundance data, we developed statistical models with relatively high explanatory power. In each case, models were improved by including vegetation-map variables, but variables directly extracted from aerial imagery were more reliable indicators of avian abundance. Although results varied by species, our models achieved reasonable within-site predictive success. When predicting to sites not used in the training set, however, validation results were inconsistent and often poor, suggesting that these models should be used with caution outside of the original study sites. As remotely sensed data become more readily available, our methods may be applied to a diverse range of sites, resulting in improved model generality and applicability.

Keywords Aerial imagery · Birds · Remote sensing · Spatial models · Wetland restoration

D. Stralberg (✉) · N. Nur
PRBO Conservation Science,
3820 Cypress Dr. #11,
Petaluma, CA 94954, USA
e-mail: dstralberg@prbo.org

M. P. Herzog
U.S. Geological Survey, Western Ecological Research Center,
Davis Field Station,
One Shields Ave., UC Davis,
Davis, CA 95616, USA

K. A. Tuxen · M. Kelly
Department of Environmental Science, Policy & Management,
UC Berkeley,
Berkeley, CA 94720, USA

Present Address:
K. A. Tuxen
Google,
1600 Amphitheatre Parkway,
Mountain View, CA 94043, USA

Introduction

The San Francisco Bay Estuary (hereafter, the Bay) is the largest estuary along the Pacific coast of North America, and at one time contained the largest contiguous tidal marsh system on the Pacific Coast (Josselyn 1983). Within the last 150 years, extensive man-made modifications of Bay habitat have taken place, accelerated by the discovery of gold in the California foothills in the mid-1800s. More than 80% of tidal wetlands have been lost as a result of human activities, such as diking, dredging, and urban development (Josselyn 1983; Nichols et al. 1986), mirroring the loss of wetlands throughout the rest of the state in that period (Dahl 1990). In addition, many remaining tidal marshes have been subdivided and altered hydrologically by levees, mosquito control ditches, board-

walks, and power lines (Boumans et al. 2002). In response to this historic loss of tidal marsh habitat, and to aid the recovery of several threatened and endangered marsh species, tidal marsh restoration in the Bay has increased dramatically in recent years. In addition to the public acquisition of 10,000 ha of salt evaporation ponds for restoration to tidal marsh habitats, over 100 other wetland restoration projects have been completed or planned in the Bay (http://www.wetlandtracker.org/ba/).

While common strategies, monitoring methods, and success criteria for tidal marsh restoration have yet to be agreed upon (Zedler 1996), many researchers and wetland practitioners agree that adaptive management is key to restoration success (Weinstein et al. 2001). Because restoration trajectories do not always follow predictable paths (Zedler and Callaway 1999), strategic monitoring and assessment are necessary. Traditional field-based monitoring generally consists of point- or transect-based samples (Neckles et al. 2002), which provide spatially limited snapshots of the site in question. Restoration monitoring may also benefit from the collection of aerial imagery and other remotely sensed data (Phinn et al. 1996; Hinkle and Mitsch 2005), which are spatially comprehensive, but limited to physical marsh characteristics that can be extracted from an image. The union of these two types of monitoring data via spatial predictive models can provide managers and researchers with an enhanced level of information about a particular site, and provide the ability to predict conditions at new sites.

In particular, spatial habitat relationship models for indicator species (Ozesmi and Mitsch 1997; Milsom et al. 2000) can be used to identify the biophysical features that relate to their distribution and abundance, and predict occurrence or abundance at unsurveyed locations. Habitat models can also be used to identify the relative importance of different environmental variables as spatial "indicator" metrics, which may be used in rapid assessment efforts to characterize habitat quality, and to improve our conceptual understanding of wetland processes and patterns. The best spatial metrics are those that represent key ecological processes (Turner 1989) and can be generalized across scales and extents (Wu 2004).

Many spatial habitat relationship models are based on satellite-derived habitat data—including classified landcover types, vegetation indices, and other spectral characteristics—at a 30-m pixel resolution or greater (Suarez-Seoane et al. 2002; Lawler et al. 2004; Bellis et al. 2008). But with the recent widespread availability of high resolution (1-m or finer) and/or multispectral aerial imagery, there exists a great opportunity to develop fine-scale predictive models that capture local-scale variability within the organism of interest (Kelly and Meentemeyer 2002; Wood et al. 2007). In particular, these types of imagery have been used to generate

spatially and floristically detailed maps of tidal marsh vegetation (Hirano et al. 2003; Judd et al. 2007), which may contain more useful information relating to the reproductive and foraging requirements of a species than vegetation indices such as the Normalized Difference Vegetation Index (NDVI). NDVI is a relatively simple way to capture the spatial heterogeneity of aboveground vegetation productivity (Kerr and Ostrovsky 2003). Through its strong correlation with aboveground net primary productivity and absorbed photosynthetically active radiation, NDVI provides an index of ecosystem function, and as such has been used in a number of habitat suitability models for a range of taxa, including insects (Estrada-Pena 1999; Shochat et al. 2004), mammals (Marshal et al. 2006; Wiegand et al. 2008), and birds (Aldridge and Boyce 2007; Brotons et al. 2007).

Breeding bird (passerine and rail) species breeding in San Francisco Bay tidal marshes have been shown to respond to individual tidal marsh plant species in addition to vegetation structure (Spautz et al. 2006), suggesting that detailed vegetation maps may be useful for predicting their distribution and abundance. While Spautz et al. (2006) identified vegetation associations for these species based on field-collected vegetation data, such detailed datasets are not available for spatial prediction across extensive areas. Additionally, it is unclear how these field-intensive parameters correspond with remotely sensed vegetation and geomorphic metrics.

Thus, we developed fine-scale spatial models of habitat relationships for three breeding tidal marsh bird species at six study sites, spanning a large salinity and geographic gradient, and including both restoration and reference sites. The study was conducted as part of a multi-disciplinary wetlands monitoring and research program for the north San Francisco Bay called the Integrated Regional Wetlands Monitoring (IRWM) program (http://www.irwm.org), the goals of which were to understand wetland ecological processes, especially in a restoration context, and identify appropriate indicators for monitoring restoration progress.

Due to the harsh environment created by high salinity and tidal inundation regimes, as well as the low structural diversity of these systems, tidal marshes are generally characterized by low vertebrate species diversity and a high proportion of endemic subspecies (Basham and Mewaldt 1987; Greenberg and Droege 1990; Greenberg et al. 2006b). Thus, the bird species that we chose for modeling are all tidal marsh-dependent species of conservation concern: tidal marsh song sparrow (*Melospiza melodia samuelis* [San Pablo Bay] and *M.m. maxillaris* [Suisun Bay and western Delta]), salt marsh common yellowthroat (*Geothlypis trichas sinuosa*), and California black rail (*Laterallus jamaicensis cotorniculus*). The song sparrow and common yellowthroat subspecies are tidal marsh endemics found primarily in San Francisco

Bay tidal marshes (Marshall and Dedrick 1994); both are California Bird Species of Special Concern (Gardali and Evens 2008; Spautz and Nur 2008a, b). The black rail is listed by the state of California as a threatened species, and more than 80% of its population is thought to be contained in northern San Francisco Bay tidal marshes (Evens et al. 1991). Perhaps due to restoration and conservation efforts, black rail and common yellowthroat populations increased from 1996 to 2008, although song sparrow (*M. m. samuelis, M.m. maxillaris*) populations have exhibited recent declines (Nur et al., PRBO Conservation Science, unpublished data).

Our specific objectives were to: (1) develop spatial models to predict avian abundance within and among marsh sites; (2) compare model predictive abilities across bird species; (3) identify fine-scale indicator metrics from remotely sensed imagery that can be used to predict patterns of abundance; (4) evaluate the importance of classified vegetation maps vs. simple geomorphic maps for prediction; and (5) compare within-site and across-site predictive abilities.

Methods

Study Area

Six tidal marshes within the North San Francisco Bay (San Pablo Bay) and western Sacramento-San Joaquin Delta were chosen as intensive study sites for multidisciplinary collaborative research efforts (Fig. 1). The six study sites consisted of two reference marshes, comprised partially or entirely of ancient (>1,000 years old) tidal marsh (SFEI
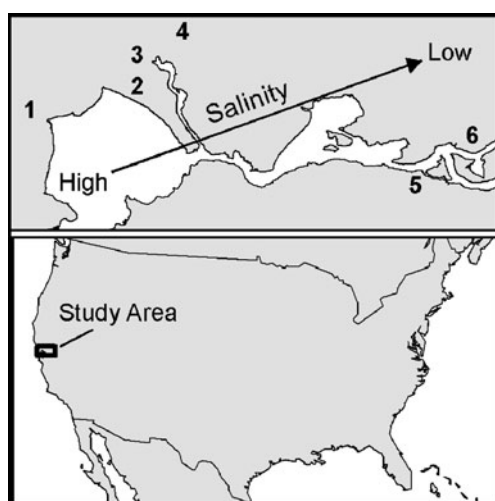

Fig. 1 Marsh study site locations. 1=Petaluma River Marsh (PRM; restoration), 2=Pond 2A (PTAR; restoration), 3=Coon Island (COIS; reference), 4=Bull Island (BUIS; restoration), 5=Browns Island (BRIS; reference), 6=Sherman Island (SHIS; restoration)

1998), and four restoration sites, ranging in age from 8 to 78 years old at the project's inception in 2003.

Aerial Imagery Acquisition

As part of the IRWM project, we obtained high-resolution color infrared aerial imagery flown at mid tide for each study site in October 2003 and August 2004 (at the end of the growing season, to maximize vegetation biomass). Aerial photographs were flown at a scale of 1:9,600 and scanned at a resolution of 1,200 dpi to achieve a pixel resolution of 0.2 m. Aerial control points were laid out in the marshes, and used to ortho-rectify the scanned photo images using ENVI photo processing software, version 3.6 (ITT 2003). RMSE values for 2004 averaged 0.233 and ranged from 0.160 to 0.368 (*n*=13 photos).

Vegetation Mapping

Images were resampled from 0.2 m to 1.0 m pixel size, in order to reduce image size for analysis and classification. All image analyses was performed with Erdas Imagine software (Leica Geosystems Inc. 2006). First, vegetated and non-vegetated areas were separated using the Normalized Difference Vegetation Index (NDVI). Next, a set of known vegetation points were used as training samples. Each vegetation group image was classified based on its training samples using a maximum likelihood classifier (MLC) supervised classification. This step rendered classified outputs for each vegetation group, which were combined together and with the non-vegetated areas (bare ground and water), to form a complete vegetation map for each site. At this point, all tiles (if more than one) were mosaicked together. Finally, the vegetation maps were smoothed using an elimination filter, resulting in a minimum mapped unit of approximately 4 m^2. Map accuracies based on independent vegetation data ranged from 70% to 91%.

Plant species composition varied by site and included Pacific cordgrass (*Spartina foliosa*), common perennial pickleweed (*Sarcocornia pacifica*), annual pickleweed (*Salicornia depressa*), alkali bulrush (*Bolboschoenus maritimus*), three-square common bulrush (*Schoenoplectus americanus*), common tule (*S. acutus* var. *occidentalis*), tule/bulrush (*S. californicus*), three cattail species (*Typha angustifolia*, *T. domengensis*, and *T. latifolia*), perennial pepperweed (*Lepidium latifolium*), alkali common reed, (*Phragmites australis*), and gumplant (*Grindelia stricta* var. *stricta*).

Geomorphic Mapping

Polygon geomorphic maps, derived from the non-vegetated portions of the 2003 vegetation maps, were complemented

by manually digitized lines representing first-order channels that were difficult to extract from the aerial imagery via automated methods. A channel centerline layer was also extracted manually from the smoothed polygons. Channel lines were digitized on-screen from 2003 aerial photos using stream mode digitizing with the same scale (1:600) and tolerance settings that were used to edit the polygons. Linear channel segments were also attributed with respect to width class.

Generation of Spatial Metrics

Based on 2004 1-m vegetation grid layers for each site, moving window metrics were calculated using the Frag-Stats software package (McGarigal and Marks 1995) and a circular, 50-m radius moving window. Moving-window vegetation metrics included proportion of each vegetation type, Shannon-Wiener diversity index, and mean NDVI value.

Based on 2004 1-m grid representations of the 2003 polygon geomorphology layers for each site, as well as line representations of the linear channel networks, circular moving-window geomorphic metrics were calculated using the neighborhood statistics and linear density functions in the ArcGIS 9 Spatial Analyst extension (ESRI 2005). Metrics calculated were linear channel density (m of channel length/m^2 of total area) and areal channel proportion. The radius used was 50 m, and outputs were 1-m grid layers. An inverse-weighted channel proximity metric—1/(distance [m] to nearest "open" [not vegetation-covered] channel)—was also calculated using the distance (straight line) and raster calculator functions in the ArcGIS 9 Spatial Analyst extension (ESRI 2005).

Finally, we calculated an inverse-weighted levee proximity metric—1/(distance [m] to nearest levee)—based on site boundaries digitized from 2003 aerial photos using ArcGIS 9.1 (ESRI 2005). Only levee boundaries for our study sites were used to develop this metric. For the site with no surrounding levees (Brown's Island) this variable was assigned a value of 0 for all pixels.

Avian Data Collection

To estimate passerine (song sparrow and common yellowthroat) abundance, we conducted five-minute point-count surveys (Ralph et al. 1993) at 90 point locations across the six study sites over a four-year period (2004–2007). We followed the same methods used by Spautz et al. (2006). All visual and auditory bird detections up to 50 m, as estimated by a trained observer

and calibrated with a rangefinder if necessary, were included in this analysis. Surveys were conducted within 4 h of sunrise, with each point visited two times between 15 March and 30 May in a given survey year. Successive survey rounds were conducted at least 3 weeks apart to minimize the effects of seasonal differences in abundance. We placed survey points 150 to 200 m apart along transects, with a randomly chosen start location and one to 20 points per site, depending on marsh size. Some points were placed along levees or boardwalks to improve sampling efficiency, but we also placed multiple points within the marsh vegetation to reduce the bias related to sampling from habitat edges.

Black rail surveys were conducted from 2004 through 2006 at 76 points, 61 of which overlapped with passerine point counts, during the breeding season between 1 April and 30 May. Surveys were conducted following a standardized tape call-back/response protocol (Evens et al. 1991; Nur et al. 1997). We summarized the data by counting the number of rails detected within 50 m, which is considered the maximum distance at which black rails can be reliably counted (Spear et al. 1999).

Model Development

Our preliminary list of spatial metrics was comprehensive, including all vegetation, geomorphology, and levee-proximity variables that were calculated (Table 1). To account for broad-scale variation among sites, we also included variables representing general physical characteristics measured in the field at the subsite level (2–5 subsites per site, delineated based on natural differences in vegetation, S. Siegel, unpubl. data): mean salinity (PSU), age (time since restoration or approximate marsh age [estimated as 1,000+ years for ancient marshes; 100 years for centennial marshes formed by Gold-Rush-era hydraulic mining sediments (Atwater et al. 1979)]), and mean elevation (m). Although this initial list of variables was informed by our a priori knowledge of tidal marsh systems and the components that are important to breeding birds, we did not constrain our analysis by pre-selecting variables for model inclusion. Because we were interested in identifying predictive spatial metrics, we did not want to bias the outcome or limit the variables unnecessarily. Rather, we conducted an exploratory analysis of univariate relationships between spatial vegetation and geomorphic metrics and bird abundance using generalized additive models (Hastie and Tibshirani 1990), which was intended (a) to modestly reduce the number of variables considered for each species and (b) to identify the most appropriate variable transformations.

Table 1 Description of geomorphic and vegetation spatial metrics evaluated for model inclusion. Metrics were calculated at the 1-m pixel level for each study site. *=within 50-m radius

Variable	Type	Definition
Site	site	Marsh site (Fig. 1): PRM, PTAR, COIS, BUIS, BRIS, COIS
SalinMean	sub-site	Mean soil water salinity (PSU)
ElevMean	sub-site	Mean marsh plain elevation (m)
AgeLn	sub-site	Log-transformed marsh age (years since restoration for restored marsh; 100 years for centennial marsh; 1000 years for ancient marsh)
LevProx	edge	Inverse distance to nearest levee (0 if no adjacent levee); levee proximity
ChArea50	geomorphic	Channel area (proportion) *
ChDens50	geomorphic	Linear channel density (m/m^2) *
ChProx	geomorphic	Inverse-weighted distance to nearest open channel; channel proximity
NDVI	vegetation	Normalized difference vegetation index; vegetation productivity *
ShDiv	vegetation map	Shannon vegetation diversity index *
SaPa	vegetation map	*Sarcocornia pacifica* (perennial pickleweed) proportion *
ScAm	vegetation map	*Schoenoplectus americanus* proportion *
BoMa	vegetation map	*Bolboschoenus maritimus* proportion *
LeLa	vegetation map	*Lepidium latifolium* (perennial pepperweed) proportion *
PhAu	vegetation map	*Phragmites australis* proportion *
SAcCa	vegetation map	*Schoenoplectus acutus/S. californicus* (tule) proportion *
SpFo	vegetation map	*Spartina foliosa* (Pacific cordgrass) proportion *

Based on bird data from all four years (2004–2007), we ran generalized additive mixed models (GAMM) with a site random effect for each species and each vegetation and geomorphic metric, using the 'mgcv' package (Wood 2006) for R (R Development Core Team 2007). Smoothing parameters for penalized regression splines were estimated using the default generalized cross validation criterion (Wood 2004). For common yellowthroat and black rail, we assumed a negative binomial distribution with a log link function; for song sparrow, we assumed a normal distribution with a linear link function. For consistency in this exploratory analysis, the dependent variable for all species was the average number of individuals detected per point (within 50 m) in a given year. For each species, we reduced the number of candidate vegetation and geomorphic variables by eliminating those without substantial indication of a relationship with bird abundance ($P>0.10$) based on the univariate GAMM model. Visual inspection of GAMM response curve plots was used to identify appropriate forms of the independent variables (i.e., linear, log, or quadratic). Physical (subsite-level) and edge (pixel-level) variables were also included in their original form as candidate variables for all species' models.

For each species, we then identified all possible generalized linear models (GLM) of point-level abundance or occurrence (see below) based on the set of candidate variables. Because we assumed that differences in bird abundance across sites were due to the unique physical characteristics of the sites themselves (e.g., site history, configuration, and surrounding land use), rather than spatial dependence within sites, we chose to specify site as a fixed, rather than random, effect in our models. We also constructed models without site terms for comparison purposes, to gain a better understanding of the vegetation and geomorphic variables that help explain differences among sites, and to facilitate prediction to sites not previously surveyed. To assess the relative importance of variables derived from classified vegetation maps, we constructed all possible models for the following nested subsets of the candidate variables using the R statistical program (R Development Core Team 2007):

1. Complete without site: all vegetation, geomorphic, and sub-site variables
2. Complete with site: as above+site term
3. Geomorphic without site: all variables not derived from classified vegetation maps
4. Geomorphic with site: as above+site term

To assess the importance of each variable, we determined a weighted deviance contribution value for each variable (by species). We did this by calculating the deviance explained by each variable in each model (the difference in model deviance with and without that variable), then multiplied those deviance contribution

values by the model's Akaike's Information Criterion (AIC) weight (w_i)—a relative measure of model support that sums to 1 across models (Burnham and Anderson 2002)—and then summed over all models (subsets 1 and 2 above). Weighted deviance contribution values for each variable were compared against χ^2 critical values for α=0.05 (11.07 for site variable [5 df], 3.84 for all other variables [1 df]), as well as AIC-based model inclusion thresholds (10 for site variable, 2 for all other variables), to determine the variable's importance across models (Lebreton et al. 1992).

For song sparrow, the dependent variable was mean annual abundance; we assumed a normal distribution with a linear link function based on the original data distribution. For common yellowthroat and black rail, the data suggested that a negative binomial distribution with a log link function would be more appropriate (Hilbe 2007). Due to the integer requirement for the dependent variable in a negative binomial model, we used the total number of detections at a point across multiple visits (with number of visits as a covariate in the model) rather than a mean abundance value.

Model Validation

Model predictive ability was first evaluated using six-fold cross-validation. We selected a different random sample of 5/6 of the survey points (across all six sites) for each of six trials, and generated predictions of each species at the remaining 1/6 of the points using model-averaged predictions from all models within 2 AIC units of the model with the lowest AIC value (following Burnham and Anderson 2002). For each of the six trials, we calculated model explanatory power (R^2 or pseudo-R^2) for predicted versus observed values (from test data only) as a validation diagnostic.

Next we performed a site-based cross-validation on each final non-site model by holding out the data from one site at a time, building the models using data from the remaining five sites, and validating those top models on the withheld site. Model averaging procedures and validation diagnostics were the same as for the standard six-fold cross-validation.

Spatial Prediction

To develop model-averaged spatial predictions for each study site, separate raster layers (in ascii grid format) for each model variable and each site, were imported to R and used as inputs for model prediction. The set of top models (ΔAIC <2) including a site term for each species were used to generate model-averaged predictions for each site based on the values of the raster layers. Pixel-level abundance predictions were converted back to ascii grids and mapped

in ArcGIS 9.2 (ESRI 2006). For common yellowthroat and black rail, we divided by the total number of visits to obtain a per-visit abundance prediction.

Model-averaged coefficients and standard errors were calculated based on the set of top models for each species, following Burnham and Anderson (2002). We considered all variables to be present in all models considered, thus setting coefficients equal to zero for models in which they were not included. Standard errors were calculated using the unconditional variance estimator based on Akaike weights (Burnham and Anderson 2002, eqn. 4.9).

Results

Univariate GAMM analysis resulted in 8 candidate vegetation and geomorphic variables for song sparrow models, 8 variables for common yellowthroat, and 10 variables for black rail (Table 2), in addition to a site term and the physical sub-site and levee-proximity variables.

Common Yellowthroat

For common yellowthroat, model explanatory power was high (partly due to the inclusion of number of survey visits as a covariate), with pseudo-R^2 values ranging from 0.75 to 0.83 for the top models in each of the four categories: complete, complete+site, geomorphic, geomorphic+site (Table 3). Based on AIC, the models with greatest support were those that included vegetation variables ("complete" models), with the best models also including a site term. Overall cross-validation yielded very good correspondence between predicted and observed abundance, especially for the top "geomorphic" models with a site term, with a mean R^2 value of 0.75 (Table 3). When cross-validation was performed by site, however, mean R^2 values were markedly lower, and variability was proportionately higher.

In terms of variable importance, levee proximity (LevProx) had the highest weighted deviance contribution, but only when the site term was not included (Fig. 2a). Other important variables in models without a site term were *Schoenoplectus acutus/S. californicus* proportion (SAcCa), channel density within 50 m (ChDens50), vegetation productivity (NDVI), and *Bolboschoenus maritimus* proportion (BoMa). The effect of levee proximity was negative, while the effects of other important variables were positive or quadratic (Supplementary Table 1).

When present, the site term had a very large weighted deviance contribution compared to other variables, although channel density, *Schoenoplectus acutus/S. californicus* proportion and *Lepidium latifolium* proportion were also important predictors in models with a site term (Fig. 2b). Both vegetation variables had positive effects (Supplementary Table 1).

Table 2 Candidate variables and transformations for inclusion in generalized linear models (by focal species). Variables are defined in Table 1; "lin"=linear; "log"=natural log; "quad"=quadratic; "sqrt"=square-root

Variable	Type	Common yellowthroat	Song sparrow	Black rail
Site	site	categorical	categorical	categorical
AgeLn	sub-site	lin	lin	lin
SalinMean	sub-site	lin	lin	lin
ElevMean	sub-site	lin	lin	lin
LevProx	edge	lin	lin	lin
ChArea50	geomorphic	quad	sqrt	lin
ChDens50	geomorphic	lin	–	lin
ChProx	geomorphic	log	log	lin
NDVI	vegetation	lin	quad	quad
ShDiv	vegetation map	quad	log	lin
SaPa	vegetation map	–	quad	lin
ScAm	vegetation map	–	log	lin
BoMa	vegetation map	quad	–	lin
LeLa	vegetation map	quad	quad	log
PhAu	vegetation map	–	–	lin
SAcCa	vegetation map	lin	log	–
SpFo	vegetation map	–	–	lin
# of candidate models	with (without) site term	82,944 (41,472)	27,648 (13,824)	196,608 (98,304)

Model-averaged predictions for mean common yellow-throat abundance ranged from nearly 0 to 5.25 birds per 50-m-radius point-count survey area (0.785 ha), and were more variable across than within sites (Figure 3a). Predicted presence was generally highest at the low-salinity sites.

Song Sparrow

For song sparrow, model explanatory power was reasonably high, with an R^2 value of 0.54 for the top model (Table 3).

Based on AIC, the models with the greatest support included a site term and vegetation variables. The top "geomorphic" model with a site term was similar in AIC to the top "complete" model without a site term. Overall cross-validation yielded reasonable correspondence between predicted and observed abundance, with best results for the top "geomorphic" models with a site term, which had a mean R^2 value of 0.44 (Table 3). When cross-validation was performed site by site, mean R^2 values were much lower.

Table 3 Model diagnostics for common yellowthroat (COYE), song sparrow (SOSP), and black rail (BLRA) top models. Complete=all vegetation, geomorphic and sub-site variables; complete with site=as above+site term; geomorphic=all variables not derived from classified vegetation maps; geomorphic with site=as above+site term

| Species	n	R^2/Pseudo-R^2	AIC	Model	Cross-validation R^2 (mean±SD)	Site validation R^2 (mean±SD)
COYE	90	0.832	271.2	Complete+Site	0.628 (±0.168)	N/A
		0.812	275.1	Complete	0.644 (±0.202)	0.363 (±0.202)
		0.809	278.2	Geomorph+Site	0.746 (±0.0426)	N/A
		0.750	295.1	Geomorph	0.609 (±0.115)	0.352 (±0.177)
SOSP	90	0.543	410.1	Complete+Site	0.392 (±0.183)	N/A
		0.454	416.0	Geomorph+Site	0.442 (±0.133)	N/A
		0.401	416.4	Complete	0.341 (±0.173)	0.159 (±0.195)
		0.191	437.4	Geomorph	0.190 (±0.169)	0.132 (±0.116)
BLRA	76	0.625	312.0	Complete+Site	0.340 (±0.272)	N/A
		0.467	319.1	Complete	0.260 (±0.188)	0.140 (±0.425)
		0.482	322.6	Geomorph+Site	0.195 (±0.127)	N/A
		0.393	322.6	Geomorph	0.198 (±0.123)	0.168 (±0.157)
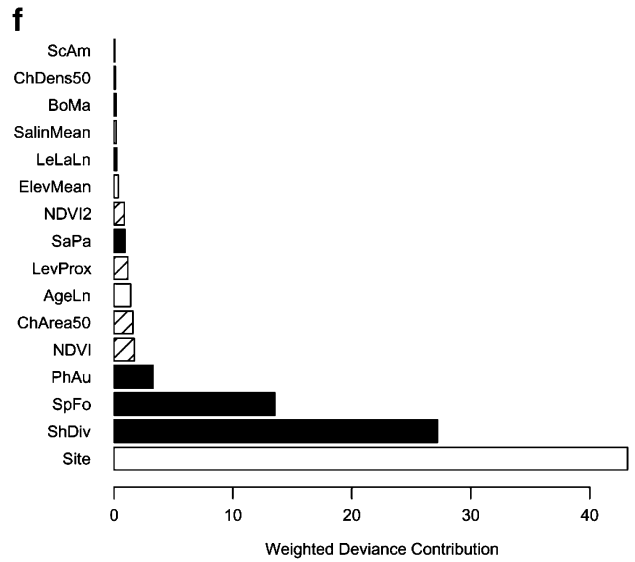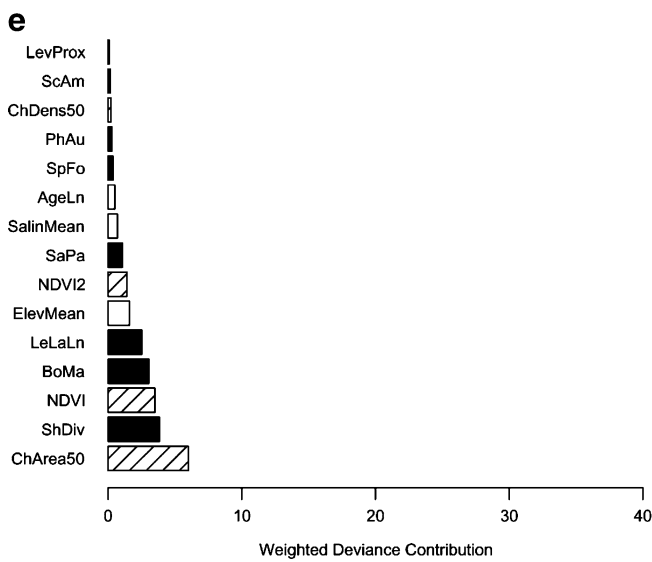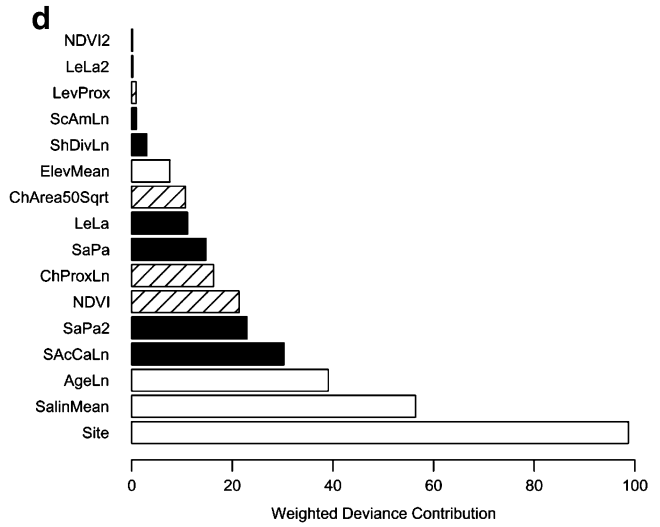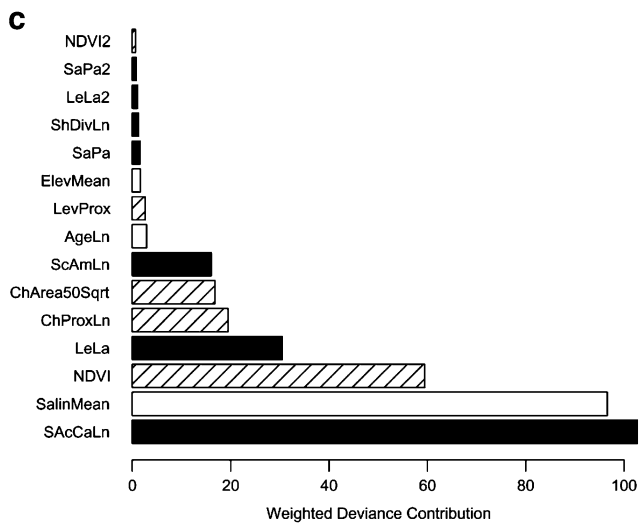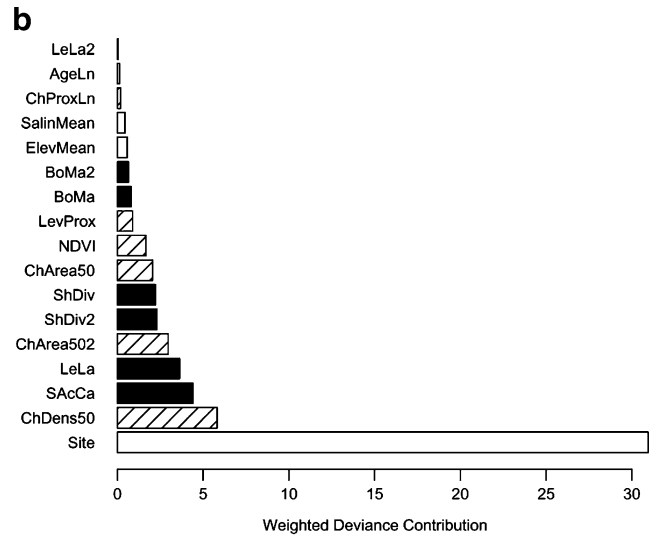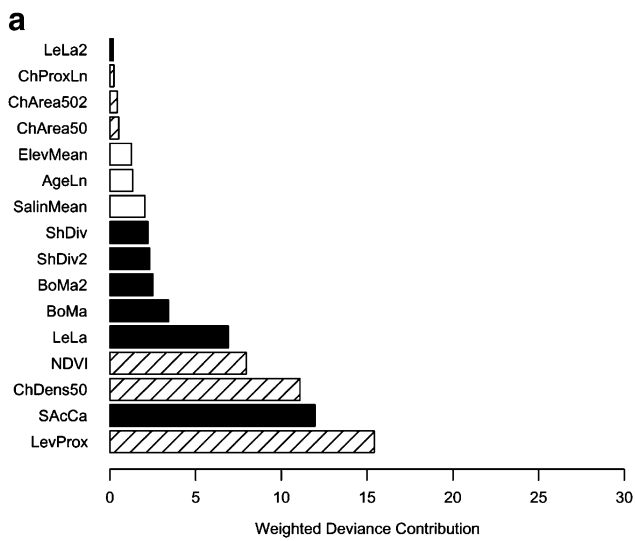
◀ **Fig. 2** Weighted deviance explained in complete common yellow-throat models, without (**a**) and with (**b**) a site term; song sparrow models, without (**c**) and with (**d**) a site term; black rail models without (**e**) and with (**f**) a site term. See Table 1 for variable descriptions ("Ln"=natural log; "2"=quadratic; "Sqrt"=square-root). Black bars represent vegetation variables; hatched bars represent geomorphic and NDVI variables; white bars represent subsite and survey variables. The Chi-square critical value for $\alpha=0.05$ and df=1 (all variables except site term) is 3.841; the Chi-square critical value for $\alpha=0.05$ and df=5 (site term) is 11.07

The variable with the highest weighted deviance contribution in the non-site models was *Schoenoplectus acutus/S. californicus* proportion (SAcCaLn), followed by mean soil salinity (SalinMean) and vegetation productivity (NDVI) (Fig. 2c). Other variables with significant weighted deviance contributions to the no-site models included *Lepidium latifolium* proportion (LeLa), channel proximity (ChProxLn), channel area (ChArea50Sqrt), and *Scirpus americanus* proportion (ScAmLn). All variables had positive effects, except *Scirpus americanus* proportion (Supplementary Table 1).

When a site term was included it had the highest weighted deviance contribution, followed by mean salinity and marsh age (AgeLn). Other variables with significant weighted deviance contributions in the presence of a site term were *Schoenoplectus acutus/S. californicus* proportion, *Sarcocornia pacifica* proportion (SaPa2 and SaPa), vegetation productivity, channel proximity, *Lepidium latifolium* proportion, channel area, mean elevation (ElevMean), and vegetation diversity (ShDivLn) (Fig. 2d). All variables had positive or quadratic effects except marsh age, mean marsh elevation, and vegetation diversity (Supplementary Table 1).

Model-averaged predictions for mean song sparrow abundance ranged from 0 to 31.6 birds per 50-m-radius point-count survey area (0.785 ha) (Figure 3b), and were more variable within than across sites.

Black Rail

For black rail, model explanatory power was fairly high (partly due to the inclusion of number of survey years as a covariate), with an R^2 value of 0.63 for the top model (Table 3). Based on AIC, the best models included vegetation variables and a site term. The top "complete" models without a site term had greater support than the top "geomorphic" models with a site term. Overall cross-validation demonstrated reasonable correspondence between predicted and observed abundance for "complete" models with a site term (mean $R^2=0.34$), but poor prediction success for "geomorphic" models and "complete" models without a site term (Table 3). When cross-validation was performed by site, mean R^2 values were much lower and highly variable.
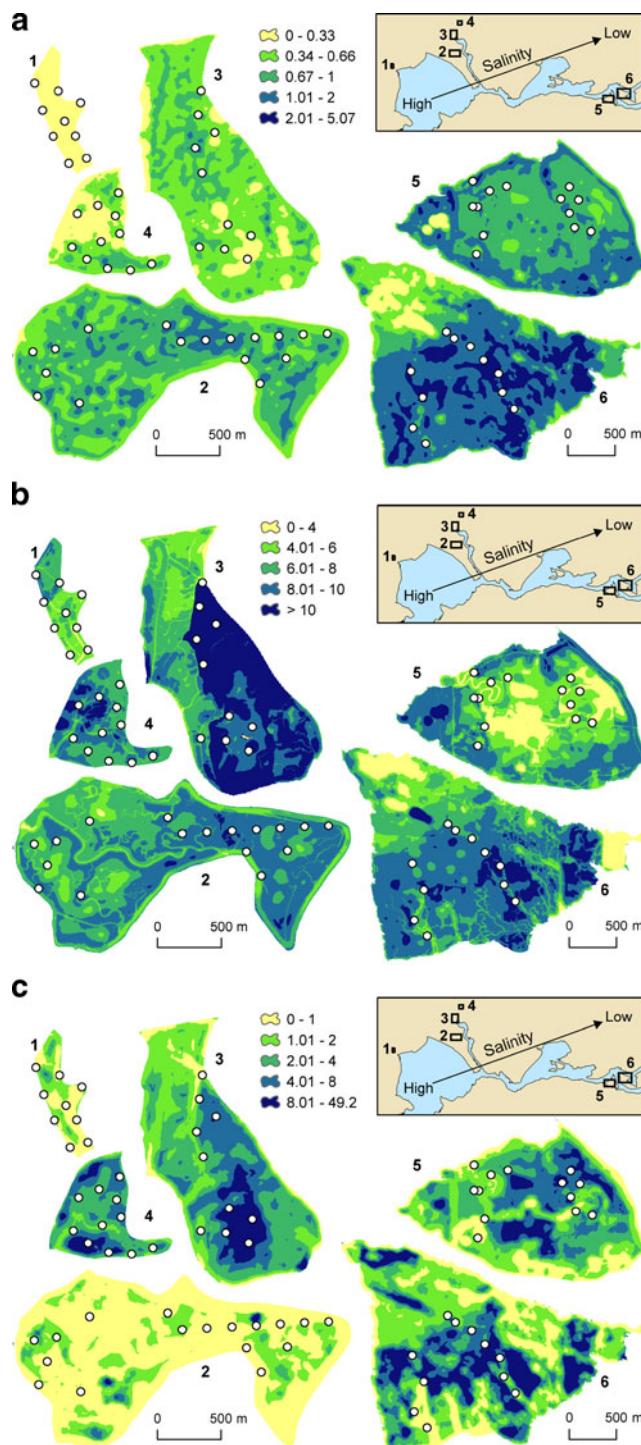

Fig. 3 Model-averaged (AIC-weighted) predicted mean abundance per 0.785 ha, based on top (delta AIC < 2) complete models (including site term) for **a** common yellowthroat, **b** song sparrow, and **c** black rail

When a site term was not included, other variables of importance were channel area (ChArea50), vegetation diversity (ShDiv), vegetation productivity (NDVI), *Bolboschoenus maritimus* proportion (BoMa), and *Lepidium latifolium* proportion (LeLaLn) (Fig. 2e). In all of the top

models, the effects of channel area, vegetation diversity, and *Bolboschoenus maritimus* proportion were negative, while the effect of *Lepidium latifolium* proportion was positive, and the effect of vegetation productivity was positive or quadratic (Supplementary Table 1).

When the site term was included, it had the highest weighted deviance contribution, followed by vegetation diversity, *Spartina foliosa* proportion (SpFo), and *Phragmites australis* proportion (PhAu) (Fig. 2f). The directions of variable effects within the top models were the same with as without a site term (Supplementary Table 1). The effect of *Phragmites australis* proportion was negative, while that of *Spartina foliosa* proportion was positive.

Model-averaged predictions for black rail abundance ranged from 0.028 to 49 birds per 50-m-radius survey area (Figure 3c). Within- and among-site variation was similar, with predicted abundance lowest at the two highest salinity sites (both restored marshes).

Discussion

Model Performance

Across all three avian species, we were able to develop predictive models with relatively high explanatory power based on aerial imagery-derived spatial metrics. For each species, model explanatory power was improved by including variables based on mapped vegetation classes, although these "complete" models did not always perform better, in terms of cross-validation results, than models containing only geomorphic variables and general sub-site conditions. While some individual vegetation variables were superseded by site-level differences (and thus dropped from models that included site terms), they are still likely to be biologically meaningful drivers of avian abundance, and useful for predicting at new sites.

This result was not unexpected, given the importance of vegetation composition and structure for breeding passerines and rails (Spautz et al. 2006), but demonstrates the ability of high-resolution aerial imagery to capture fine-scale differences in vegetation that affect breeding bird abundance and distribution. This is one of very few applications of fine-scale aerial imagery-derived vegetation GIS data to predict wildlife abundance and distribution (but see Wood et al. 2007), and is the only such known example for marsh breeding birds.

Species Differences

Although some predictor variables were shared across species, our models highlight the complementary and unique habitat requirements of each species, as well as

different types of responses and potential to serve as tidal marsh indicators. For common yellowthroat, predictive ability and cross-validation success was high, but predictions varied greatly by site and mean salinity was an important predictor, suggesting that this species' abundance is driven in large part by site-level processes, more than within-site variation in vegetation and geomorphology. Song sparrow models also had good predictive ability and reasonable cross-validation success. Models for this species included more vegetation and geomorphic variables of importance, however, and resulted in predictions with greater within- than across-site variability, suggesting that the abundance of this nearly ubiquitous tidal marsh species is primarily driven by local, within-marsh processes. Results for black rail were somewhat intermediate, with models that had fairly high predictive ability but low cross-validation success, and predictions that exhibited similar within- and across-site variability. However, the low predicted abundance of this species at young restoration sites (along with its threatened population status) suggests that model results may be confounded by slow colonization of newly restored sites. Thus, the use of these three species as marsh indicators may vary according to spatial and temporal scale: short-term and local-level for song sparrow, short-term and site-level for common yellowthroat, and long-term and local- to site-level for black rail.

Indicator Spatial Metrics

The predictive abilities of the spatial indicator metrics used in this analysis varied greatly among species. Because of the large salinity gradient across which our study was conducted, none of the vegetation types examined were present at all six sites; this may have affected our ability to detect consistently strong relationships from our multi-model analysis. While many vegetation and geomorphic metrics were present in all or most of the top models used for prediction, only a few variables emerged as significant when considering the full set of AIC-weighted models. Fewer variables were important across sites (i.e., in models without a site term), most of which were not specific vegetation types. This may be related to the relatively small number of sites included in this analysis, but may also reflect interannual variation in vegetation over the four bird survey years that could not be captured by our single-year imagery-derived metrics. In addition, some important floristic and structural vegetation details are necessarily lost in any vegetation classification scheme, and some important vegetation components were not well captured by our imagery due to timing. Here we discuss just those variables that were most important for explaining variation among sites, which may have general relevance for restoration and management purposes.

Across sites, our models predicted a higher frequency of common yellowthroat detections in areas that were farther away from levees. Habitat near levees may be associated with a lack of low-marsh vegetation types known to be used by this species, such as *B. maritimus* (Spautz et al. 2006), based on the hydrologic effects of levees on marsh vegetation and channel formation. Levees may also serve as conduits for land-based predators and nest parasites (cowbirds), which could negatively affect common yellowthroat occurrence. In either case, this may be an important consideration for the management of this species, especially in the context of restoration, where levees may either be breached or removed entirely.

For both common yellowthroat and song sparrow abundance, we found strong positive or curvilinear associations with the proportions of *Schoenoplectus acutus/S. californicus* (tule) and the invasive *Lepidium latifolium* (pepperweed), which are associated with fresh and brackish marshes. Song sparrow abundance was also positively associated with salinity, however, reflecting the generalist nature of this species, which is found in a wide variety of habitats throughout North America.

Perhaps more informative and useful was the importance of vegetation productivity, as measured by NDVI, which has been positively associated with breeding bird abundance and species richness at broader spatial scales (Hurlbert 2004; Evans et al. 2006), and may reflect structural habitat availability for both of these species (as well as black rail). NDVI is derived directly from spectral properties and does not require the development of a vegetation map, which makes it a good candidate for rapid, cost-effective monitoring. Channel area (proportion), density, and proximity were also important predictors for these two species. Channel proximity has been identified as a strong predictor of vegetation diversity and composition (Sanderson et al. 2000), and may serve as a proxy for vegetation types that were not well captured by our vegetation map, such as *Grindelia stricta* (gum plant), which is used by song sparrows for nesting, and has been positively associated with the abundance of that species (Spautz et al. 2006). Channel proximity, density, and area may also affect birds directly via resource availability, predation risk, and flooding (Greenberg et al. 2006a).

For black rail, channel area (proportion) and vegetation diversity were the most consistent (negative) predictors of abundance across sites. These variables may be proxies for the high-marsh areas that this species is thought to require for nesting and to avoid exposure to predators during extreme high tide (Evens and Page 1986; Conway and Sulzman 2007). While marsh age and mean elevation (at the sub-site level) were present as positive predictors in many of the top models, the resolution of these data was not great enough to capture within-site variation.

Model Generality

Our models achieved moderate to high within-site predictive success with data from just six sites. For all species, however, the inclusion of a site term generally improved model explanatory power and affected the importance of other variables when included. This reflects the high variability among our study sites, and suggests the importance of other unknown variables associated with individual sites, such as site history and land use, which may affect site vegetation and geomorphology in ways that we did not measure, but may also affect biotic interactions via prey resources and predator communities.

When predicting to new sites not in the training dataset, results were generally inconsistent, and often poor. The large variation in predictive success suggests that these models should be used with caution outside of the original study sites. Given the relatively small number of sites surveyed, and the large variation among them, this is not a surprising result. The collection of new data from additional sites could help improve our models and their validation success. As with any system, field survey locations should be strategically placed to encompass a broad range of conditions and thus improve model predictive power. As high-resolution imagery and derived vegetation maps become more readily accessible for large, diverse areas such as the San Francisco Bay, our approach should result in increasingly robust, general models with greater direct applicability.

Implications for Wetland Restoration and Monitoring

This study highlights the importance of high-resolution, remotely-sensed vegetation data for monitoring natural and restored tidal marshes, not just for vegetation, but also for birds and potentially other wildlife (Phinn et al. 1996). While remote sensing cannot replace on-the-ground monitoring, it can improve its efficiency, especially for large sites with limited accessibility. Aerial imagery and vegetation maps, through spatial predictive models, can be used to extend the value of field survey data. Our results also highlight the value of spectrally-derived metrics such as NDVI and geomorphic (e.g., channel) metrics, which are much easier to calculate than classified vegetation maps. Our findings suggest that such variables may be better (and cheaper) indicators for birds than specific plant information from classified vegetation maps.

Finally, we should emphasize that it is important to exercise caution in the extrapolation of models to new sites, especially if conditions differ greatly from model-building sites. Restoration monitoring is an adaptive process, whereby new information should be continually incorporated as it becomes available (Weinstein et al. 2001). A single model

does not provide a conclusive answer, and should be treated as a working hypothesis that can be iteratively refined.

References

Aldridge CL, Boyce MS (2007) Linking occurrence and fitness to persistence: Habitat-based approach for endangered greater sage-grouse. Ecological Applications 17:508–526

Atwater BF, Conrad SG, Dowden JN, Hedel CW, MacDonald RL, Savage W (1979) History, landforms, and vegetation of the estuary's tidal marshes. In: Conomos TJ (ed) San Francisco Bay: The urbanized estuary. American Association for the Advancement of Science, San Francisco, pp 347–386

Basham MP, Mewaldt LR (1987) Salt water tolerance and the distribution of South San Francisco Bay Song Sparrows. Condor 89:697–709

Bellis LM, Pidgeon AM, Radeloff VC, St-Louis V, Navarro JL, Martella MB (2008) Modeling habitat suitability for greater rheas based on satellite image texture. Ecological Applications 18:1956–1966

Boumans RMJ, Burdick DM, Dionne M (2002) Modeling habitat change in salt marshes after tidal restoration. Restoration Ecology 10:543–555

Brotons L, Herrando S, Pla M (2007) Updating bird species distribution at large spatial scales: Applications of habitat modelling to data from long-term monitoring programs. Diversity and Distributions 13:276–288

Burnham KP, Anderson DR (2002) Model selection and multimodel inference: A practical information-theoretic approach. Springer-Verlag, New York

Conway CJ, Sulzman C (2007) Status and habitat use of the California Black Rail in the southwestern USA. Wetlands 27:987–998

Dahl TE (1990) Wetlands losses in the United States 1780's to 1980's. U.S. Department of the Interior, Fish and Wildlife Service, Washington, DC. http://www.npwrc.usgs.gov/resource/wetlands/wetloss/index.htm. Accessed 23 Nov 2009

ESRI (2005) ArcGIS 9.1. Environmental Systems Research Institute, Redlands, CA

ESRI (2006) ArcGIS 9.2. Environmental Systems Research Institute. Redlands, CA

Estrada-Pena A (1999) Geostatistics and remote sensing using NOAA-AVHRR satellite imagery as predictive tools in tick distribution and habitat suitability estimations for Boophilus microplus (Acari: Ixodidae) in South America. Veterinary Parasitology 81:73–82

Evans KL, James NA, Gaston KJ (2006) Abundance, species richness and energy availability in the North American avifauna. Global Ecology and Biogeography 15:372–385

Evens J, Page GW (1986) Predation on black rails during high tides in salt marshes. Condor 88:107–109

Evens J, Page GW, Laymon SA, Stallcup RW (1991) Distribution, relative abundance, and status of the California black rail in western North America. Condor 93:952–966

Gardali T, Evens JG (2008) Salt Marsh Common Yellowthroat, Geothlypis trichas sinuosa. In: Shuford WD, Gardali T (eds) California Bird Species of Special Concern: A ranked assessment of species, subspecies, and distinct populations of immediate conservation concern in California. Studies of Western Birds 1, Camarillo and Sacramento, CA, pp 346–350

Greenberg R, Droege S (1990) Adaptations to tidal marshes in breeding populations of the swamp sparrow. Condor 92:393–404

Greenberg R, Elphick C, Nordby JC, Djerdum C, Spautz H, Shriver G, Schmeling B, Olson B, Marra P, Nur N, Winter M (2006a) Flooding and predation: Trade-offs in the nesting ecology of tidal marsh sparrows. Studies in Avian Biology 32:96–109

Greenberg R, Maldonado J, Droege S, McDonald MV (2006b) Tidal marshes: A global perspective on the evolution and conservation of their terrestrial vertebrates. Bioscience 56:675–685

Hastie TJ, Tibshirani RJ (1990) Generalized additive models. Chapman & Hall, London

Hilbe J (2007) Negative binomial regression. Cambridge University Press, Cambridge

Hinkle RL, Mitsch WJ (2005) Salt marsh vegetation recovery at salt hay farm wetland restoration sites on Delaware Bay. Ecological Engineering 25:240–251

Hirano A, Madden M, Welch R (2003) Hyperspectral image data for mapping wetland vegetation. Wetlands 23:436–448

Hurlbert AH (2004) Species-energy relationships and habitat complexity in bird communities. Ecology Letters 7:714–720

ITT (2003) ENVI, v. 3.6. Boulder, CO

Josselyn M (1983) The ecology of San Francisco Bay tidal marshes: A community profile. FWS/OBS-83/23. U.S. Fish and Wildlife Service, Division of Biological Services, Washington, DC

Judd C, Steinberg S, Shaughnessy F, Crawford G (2007) Mapping salt marsh vegetation using aerial hyperspectral imagery and linear unmixing in Humboldt Bay, California. Wetlands 27:1144–1152

Kelly M, Meentemeyer RK (2002) Landscape dynamics of the spread of Sudden Oak Death. Photogrammetric Engineering and Remote Sensing 68:1001–1009

Kerr J, Ostrovsky M (2003) From space to species: Ecological applications for remote sensing. Trends in Ecology and Evolution 18:299–314

Lawler JJ, O'Connor RJ, Hunsaker CT, Jones KB, Loveland TR, White D (2004) The effects of habitat resolution on models of avian diversity and distributions: A comparison of two land-cover classifications. Landscape Ecology 19:517–532

Lebreton J-D, Burnham KP, Clobert J, Anderson DR (1992) Modeling survival and testing biological hypotheses using marked animals: A unified approach with case studies. Ecological Monographs 62:67–118

Leica Geosystems Inc. (2006) ERDAS Imagine

Marshal JP, Belich VC, Krausman PR, Reed ML, Andrew NG (2006) Factors affecting habitat use and distribution of desert mule deer in an arid environment. Wildlife Society Bulletin 34:609–619

Marshall J, Dedrick K (1994) Endemic song sparrows and yellow-throats of San Francisco Bay. Studies in Avian Biology 15:316–327

McGarigal K, Marks BJ (1995) FRAGSTATS: Spatial pattern analysis program for quantifying landscape structure. USDA Forest Service GTR PNW-351. http://www.umass.edu/landeco/research/fragstats/fragstats.html. Accessed 23 Nov 2009

Milsom TP, Langton SD, Parkin WK, Peel S, Bishop JD, Hart JD, Moore NP (2000) Habitat models of bird species' distribution: An aid to the management of coastal grazing marshes. Journal of Applied Ecology 37:706–727

Neckles HA, Dionne M, Burdick DM, Roman CT, Buchsbaum R, Hutchins E (2002) A monitoring protocol to assess tidal restoration of salt marshes on local and regional scales. Restoration Ecology 10:556–563

Nichols FH, Cloern JE, Luoma SN, Peterson DH (1986) The modification of an estuary. Science 231:567–573

Nur N, Zack S, Evens J and Gardali T (1997) Tidal marsh birds of the San Francisco Bay region: Status, distribution, and conservation of five Category 2 taxa. Final draft report to National Biological Survey (now US Geological Survey). Point Reyes Bird Observatory, Stinson Beach, CA. http://www.prbo.org/cms/docs/wetlands/tmreport1997.pdf. Accessed 23 Nov 2009

Ozesmi U, Mitsch WJ (1997) A spatial habitat model for the marsh-breeding red-winged blackbird (Agelaius phoeniceus L.) in coastal Lake Erie wetlands. Ecological Modelling 101:139–152

Phinn S, Stow D, Zedler J (1996) Monitoring wetland habitat restoration in southern California using airborne multispectral video data. Restoration Ecology 4:412–422

R Development Core Team (2007) R: A language and environment for statistical computing. R Foundation for Statistical Computing, Vienna, Austria

Ralph CJ, Geupel GR, Pyle P, Martin TE, DeSante DF (1993) Handbook of field methods for monitoring landbirds. PSW-GTR-144. USDA Forest Service, Pacific Southwest Research Station, Corvallis, OR. http://www.treesearch.fs.fed.us/pubs/3639. Accessed 23 Nov 2009

Sanderson EW, Ustin SL, Foin TC (2000) The influence of tidal channels on the distribution of salt marsh plant species in Petaluma Marsh, CA, USA. Plant Ecology 146:29–41

SFEI (1998) EcoAtlas beta release, version 1.5b4. San Francisco Estuary Institute, Oakland, CA. http://www.sfei.org/ecoatlas/index.html. Accessed 2 June 2008

Shochat E, Stefanov WL, Whitehouse MEA, Faeth SH (2004) Urbanization and spider diversity: Influences of human modification of habitat structure and productivity. Ecological Applications 14:268–280

Spautz H, Nur N (2008a) Suisun Song Sparrow, Melospiza melodia maxillaris. In: Shuford WD, Gardali T (eds) California Bird Species of Special Concern: A ranked assessment of species, subspecies, and distinct populations of immediate conservation concern in California. Studies of Western Birds 1, Camarillo and Sacramento, CA, pp. 405–411

Spautz H, Nur N (2008b) Suisun Song Sparrow, Melospiza melodia samuelis. In: Shuford WD, Gardali T (eds) California Bird Species of Special Concern: A ranked assessment of species, subspecies, and distinct populations of immediate conservation concern in California. Studies of Western Birds 1, Camarillo and Sacramento, CA, pp. 412–418

Spautz H, Nur N, Stralberg D, Chan Y (2006) Multiple-scale habitat relationships of tidal marsh breeding birds in the San Francisco Bay estuary. Studies in Avian Biology 32:247–269

Spear L, Terrill SB, Lenihan C, Delevoryas P (1999) Effects of temporal and environmental factors on the probability of detecting California Black Rails. Journal of Field Ornithology 70:465–480

Suarez-Seoane S, Osborne PE, Alonso JC (2002) Large-scale habitat selection by agricultural steppe birds in Spain: Identifying species-habitat responses using generalized additive models. Journal of Applied Ecology 39:755–771

Turner MG (1989) Landscape ecology: The effect of pattern on process. Annual Review of Ecology and Systematics 20:171–197

Weinstein MP, Teal JM, Balletto JH, Strait KA (2001) Restoration principles emerging from one of the world's largest tidal marsh restoration projects. Wetlands Ecology and Management 9:387–407

Wiegand T, Naves J, Garbulsky MF, Fernandez N (2008) Animal habitat quality and ecosystem functioning: Exploring seasonal patterns using NDVI. Ecological Monographs 78:87–103

Wood DJA, Drake S, Rushton SP, Rautenkranz D, Lurz PWW, Koprowski JL (2007) Fine-scale analysis of Mount Graham red squirrel habitat following disturbance. Journal Of Wildlife Management 71:2357–2364

Wood SN (2004) Stable and efficient multiple smoothing parameter estimation for generalized additive models. Journal of the American Statistical Association 99:673–686

Wood SN (2006) Generalized additive models: An introduction with R. Chapman and Hall/CRC Press, New York

Wu J (2004) Effects of changing scale on landscape pattern analysis: Scaling relations. Landscape Ecology 19:125–138

Zedler JB (1996) Coastal mitigation in southern California: The need for a regional restoration strategy. Ecological Applications 6:84–93

Zedler JB, Callaway JC (1999) Tracking wetland restoration: Do mitigation sites follow desired trajectories? Restoration Ecology 7:69–73